

# EZH2 inhibitors abrogate upregulation of trimethylation of H3K27 by CDK9 inhibitors and potentiate its activity against diffuse large B-cell lymphoma

Shao Xie,<sup>1,2,#</sup> Fan Wei,<sup>1,3,#</sup> Yi-ming Sun,<sup>1</sup> Ying-lei Gao,<sup>1</sup> Lu-lu Pan,<sup>3,4</sup> Min-jia Tan,<sup>4</sup> Shu-dong Wang,<sup>5</sup> Jian Ding<sup>1</sup> and Yi Chen<sup>1</sup>

<sup>1</sup>Division of Anti-Tumor Pharmacology, State Key Laboratory of Drug Research and Institute of Materia Medica, Chinese Academy of Sciences, Shanghai, China; <sup>2</sup>Key Laboratory of Breast Cancer, and Fudan University Shanghai Cancer Center, Fudan University, Shanghai, China; <sup>3</sup>University of Chinese Academy of Sciences, Beijing, China; <sup>4</sup>Chemical Proteomics Center, State Key Laboratory of Drug Research, Shanghai Institute of Materia Medica and Chinese Academy of Sciences, Shanghai, China and <sup>5</sup>Centre for Drug Discovery and Development, School of Pharmacy and Medical Sciences, University of South Australia Cancer Research Institute, Adelaide, Australia

<sup>#</sup>SX and FW are co-first authors.



Haematologica 2020  
Volume 105(4):1021-1031

## ABSTRACT

Aberrant expression of CDK9/cyclin T1 has been found in diffuse large B-cell lymphoma (DLBCL), and suggests that CDK9 is a potential therapeutic target for DLBCL. Here, we firstly demonstrated that CDKI-73, a novel cyclin-dependent kinases (CDK) inhibitor, potently blocks CDK9, triggered apoptosis and dramatically repressed DLBCL cell growth owing to CDK9 inhibition. CDK9 inhibitors specifically elevated the trimethylation of H3K27, which we speculate was due to reduced expression of JMJD3/UTX. Considering the important role of the trimethylation of H3K27 in tumor progression, the synergistic effect of the combination therapy of CDK9 inhibitors with EZH2 inhibitors was investigated. EZH2 inhibitors reversed the upregulation of trimethylation of H3K27, and synergistically inhibited DLBCL and other solid tumors growth *in vitro* and *in vivo*. These findings provide a rational basis for the application of CDK9 inhibitors in combination with EZH2 inhibitors in clinical trials.

## Introduction

Diffuselarge B-cell lymphoma (DLBCL) is the most common aggressive lymphoma, accounting for 30-40% of all Non-Hodgkin lymphoma incidences.<sup>1</sup> Despite the fact that the median survival time of DLBCL patients is over 8 years, more than 25-30% of the patients relapse,<sup>1</sup> making it necessary to develop more effective therapeutics.

CDK9, together with cyclin T/K, is responsible for the transcription elongation of most protein-coding genes through phosphorylating the RNA polymerase II (RNA Pol II) at the ser2 residual.<sup>2,3</sup> Similar to other lymphoma sub-types, DLBCL has a deregulated cell cycle. These alterations suggest that inhibitors of cyclin-dependent kinases (CDK) might be beneficial for patients affected by DLBCL.<sup>4</sup> Research indicates that CDK9/cyclin T1 is involved in lymphocyte differentiation and activation, and shows an aberrant expression in DLBCL.<sup>5</sup> In addition, MCL1 expression, which can be downregulated by CDK9 inhibition,<sup>6</sup> was found to be overexpressed in a significant fraction of DLBCL,<sup>6,7</sup> contributing to therapy resistance.<sup>8</sup> All these suggest that CDK9 inhibition seems to be a potential therapeutic strategy for the treatment of DLBCL.

Methylation of lysine 27 on histone H3 (H3K27me), a modification associated with gene repression, plays a critical role in regulating the expression of genes that determine the balance between cell differentiation and proliferation.<sup>9</sup> This modifi-

## Correspondence:

YI CHEN  
ychen@simm.ac.cn

JIAN DING  
jding@simm.ac.cn

Received: March 26, 2019.

Accepted: July 5, 2019.

Pre-published: July 9, 2019.

doi:10.3324/haematol.2019.222935

Check the online version for the most updated information on this article, online supplements, and information on authorship & disclosures: [www.haematologica.org/content/105/4/1021](http://www.haematologica.org/content/105/4/1021)

©2020 Ferrata Storti Foundation

Material published in Haematologica is covered by copyright. All rights are reserved to the Ferrata Storti Foundation. Use of published material is allowed under the following terms and conditions:

<https://creativecommons.org/licenses/by-nc/4.0/legalcode>. Copies of published material are allowed for personal or internal use. Sharing published material for non-commercial purposes is subject to the following conditions: <https://creativecommons.org/licenses/by-nc/4.0/legalcode>, sect. 3. Reproducing and sharing published material for commercial purposes is not allowed without permission in writing from the publisher.



cation is generated by the polycomb repressive complex 2 (PRC2), composed of the SET domain-containing histone methyltransferase EZH2, and accessory proteins EED, SUZ12.<sup>10</sup> However, the methylation of H3K27 can be removed by the histone demethylases UTX/KMD6A and JMJD3/KDM6B.<sup>11</sup> Given the critical role of the H3K27me in gene expression, it is not surprising that this chromatin modification plays a role in malignancies, such as lymphoma, breast and esophageal cancer.<sup>12</sup> Accumulating studies imply that H3K27me3 is closely engaged in the development of DLBCL, especially in the germinal center B-cell subtype,<sup>13</sup> reducing H3K27me3 level exhibits significant anti-proliferation activity against DLBCL.<sup>14</sup> Further, highly selective EZH2 inhibitors (EZH2i), such as GSK126, EPZ6438, and CPI-1205 are currently undergoing clinical evaluation against DLBCL, and show clinical efficiency by reducing the level of H3K27me3. However, clinical benefits of EZH2i remain unsatisfactory against other solid tumors.

CDKI-73 (also named LS-007, QHRD107), a novel phase I clinical stage CDK inhibitor in China, mainly targets CDK9 with sub-nanomolar biochemical potency and represses expression of MCL1 in multiple models of cancer, such as chronic lymphocytic leukemia (CLL), ovarian cancer, and acute leukemia.<sup>15-17</sup> CDKI-73 is highly cytotoxic to primary leukemia cells from CLL patients and showed >500-fold selectivity for primary leukemia cells over normal B-lymphocytes,<sup>15</sup> making it an attractive candidate for clinical development. In this study, firstly, we assessed the *in vitro* and *in vivo* activity of CDKI-73 against DLBCL. However, during the research, we found that CDKI-73 significantly elevated H3K27me3 level owing to CDK9 inhibition, accompanied with more pronounced transcriptional down-regulation of H3K27me3-targeted genes. Therefore, we hypothesized that the combined treatment of CDK9 inhibitors (CDK9i) and EZH2i would show greater antitumor activity than treatment with either inhibitor alone. We found a particularly potent synergy of this combination against both DLBCL and other solid tumors *in vitro* and *in vivo*, revealing that this potential therapeutic combination could be evaluated in patients.

## Methods

### Cell culture

All cells were purchased from ATCC (Manassas, VA, USA) or DSMZ (Brunswick, Germany) and maintained following the suppliers' instructions.

Cell proliferation, apoptosis, colony formation assay, comet assay, quantitative Real-Time PCR analysis, chemicals and antibodies were described in the *Online Supplementary Methods*.

### Mass Spectrometry (MS) of histone modifications

Histones of SU-DHL-4 cells from SILAC (stable isotope labeling by amino acids) were manipulated as previously described.<sup>18</sup> Then the peptides were separated by EASY-nLC 1000 HPLC system and analyzed using Orbitrap Fusion mass spectrometer (Thermo Fisher Scientific). MS data were analyzed by Mascot software against an in-house human histone sequence database (83 sequences; 13,870 residues) generated from the UniProt database (updated on 01/27/2015). Peptides containing modifications were manually quantified using the Qual Browser (Thermo Fisher Scientific).

### ChIP-Seq

H3K27me3 ChIP-seq data with spike-in was generated by Active Motif's Epigenetic Services team (Active Motif, CA, USA). Karpas-422 cells were harvested as previously described.<sup>19</sup> Cell pellets were snap-frozen in liquid nitrogen for 10 min, stored at -80°C and then shipped to Active Motif on dry ice for the H3K27me3 ChIP-seq assay.

### Animal experiments

All experiments were performed according to the institutional ethical guidelines on animal care and approved by the Institute of Animal Care and Use Committee at the Shanghai Institute of Materia Medica (No. 2016-04-DJ-21). Pfeiffer, SU-DHL-6 were subcutaneously injected into the right flank of SCID mice and SW620 were subcutaneously injected into the right flank of nude mice at  $5 \times 10^6$  cells/mouse (six mice per group). Tumor bearing mice were randomized into groups and started dosing when average tumor volume reached 100–200 mm<sup>3</sup>. CDKI-73 (0.5% HPMC+ddH<sub>2</sub>O) and EPZ6438 (0.5% CMCNa+1% Tween80+ddH<sub>2</sub>O) were given orally daily. For combination treatment, drugs were given concurrently. Tumors and body weight were measured twice a week, and the relative tumor volume (RTV) was calculated with the formula:  $RTV = (\frac{1}{2} \times \text{length} \times \text{width}^2 \text{ of day } n) / (\frac{1}{2} \times \text{length} \times \text{width}^2 \text{ of day } 0)$ . The therapeutic effect of the compounds was expressed as the volume ratio of treatment to control:  $T/C (\%) = 100 \% \times (\text{mean } RTV_{\text{treated}}) / (\text{mean } RTV_{\text{vehicle}})$ .

### Statistical analysis

Combination index (CI) values were calculated using CalcuSyn software or using the IC<sub>50</sub> ratio obtained with CDK9i plus EZH2i compared to that obtained with CDK9i alone as previously described.<sup>20</sup> Student's *t*-test was applied for statistical comparison using GraphPad Prism. Unless otherwise indicated, the results are expressed as the mean ± standard deviation (SD) from at least three independent experiments. Differences were considered to be statistically significant at  $P < 0.05$ .

## Results

### CDKI-73 inhibits the growth of DLBCL cells *in vitro* and *in vivo*

The activity of CDKI-73 against human DLBCL was evaluated using a panel of established DLBCL cell lines. CDKI-73 remarkably restrained the proliferation of all tested DLBCL cell lines with the mean IC<sub>50</sub> values of 87±40 nM, which was slightly lower than that of Flavopiridol, a reported potent CDK9 inhibitor (125±40 nM) (Figure 1A).

Considering that CDKI-73 has been reported to be a potent CDK9 inhibitor,<sup>15-17</sup> we investigated its influence on CDK9 activity in DLBCL cell lines. As expected, significant suppression of phosphorylation of RNA Pol II (ser2) was also found in SU-DHL-4, Pfeiffer and WSU-DLCL-2 cells treated with CDKI-73 in a dose-dependent manner (Figure 1B). As CDK9 plays a vital role in regulating the transcription of numerous anti-apoptotic proteins, its inhibition-induced cell death has been confirmed to be through apoptosis.<sup>7</sup> Therefore, we examined the effect of CDKI-73 on apoptosis. As expected, CDKI-73 led to apoptosis in three DLBCL cell lines, WSU-DLCL2, SU-DHL-4, and Pfeiffer, in a concentration- and time-dependent manner (Figure 1C). Simultaneously, PARP cleavage increased consistently with the occurrence of apoptosis

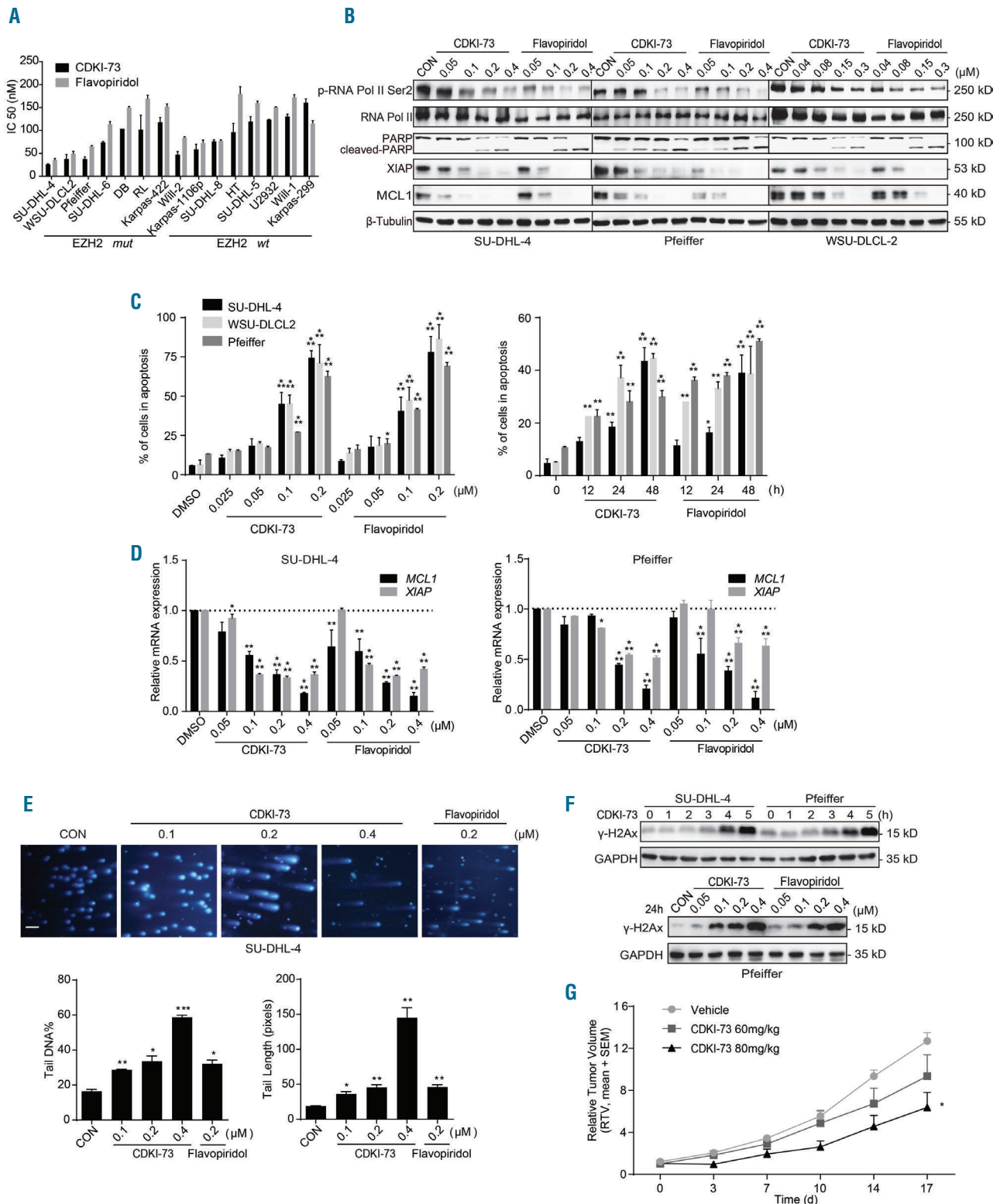


**Figure 1. Efficiency of CDK1-73 on diffuse large B-cell lymphoma cells.** (A) The IC<sub>50</sub> values of diffuse large B-cell lymphoma (DLBCL) cell lines after exposure to CDK1-73/Flavopiridol for 72 hours (h). (B) Cellular CDK9 inhibition [2 h for detection of RNA polymerase II (RNA Pol II) (ser2)] and the level of apoptosis-related proteins (24 h) influenced by CDK1-73/Flavopiridol. (C) Apoptosis caused by CDK1-73/Flavopiridol. (D) The relative mRNA expression of *MCL1* and *XIAP* after treated with CDK1-73/Flavopiridol for 6 h. (E) Comet assay. Cells were treated with CDK1-73/Flavopiridol for 24 h (scale bar, 25 μm). Quantified results of the average DNA contents and the length of the comet tails using CometScor software. (F) γ-H2AX level in Pfeiffer and SU-DHL-4 cells treated with indicated time or dose of CDK1-73/Flavopiridol. (G) Tumor growth curve graphs RTV over time in each treatment group in Pfeiffer xenografts. Data are expressed as the mean + standard error of the mean (SEM). All data are representative of at least three independent experiments. \*\*\**P*<0.001, \*\**P*<0.01, \**P*<0.05 compared with the control group. Mut: mutant; wt: wild-type.

(Figure 1B). Further, we assessed the impact of CDKI-73 on the expression of anti-apoptotic proteins MCL1 and XIAP, which were proved to be down-regulated by CDK9 inhibition.<sup>7</sup> Both SU-DHL-4 and Pfeiffer cells exposed to increasing doses of CDKI-73 exhibited decreased levels of MCL1 and XIAP at both protein (Figure 1B) and mRNA levels (Figure 1D), indicating transcriptional inhibition. The pattern is similar to that of Flavopiridol. These results indicated that CDKI-73 inhibits CDK9 activity efficiently in DLBCL cell lines.

In addition to its predominant participation in transcription, CDK9 also acts as a DNA damage response-related protein.<sup>21</sup> CDK9/cyclin K is directly involved in maintaining the genomic integrity.<sup>21</sup> Hence, we assessed the ability of CDKI-73 in inducing DNA damage in DLBCL cells. Both comet assay and  $\gamma$ -H2AX analysis indicated that CDKI-73 could induce DNA double strand breaks (DSB) in a dose- and time-dependent manner, as evidenced by the elevation of  $\gamma$ -H2AX expression, the frequent appearance and expanding volume of comet tails, as well as the shrinkage of comet heads (Figure 1E-F).

The results listed above show that CDKI-73 can potentially inhibit the *in vitro* proliferation of DLBCL. Subsequently, the *in vivo* effect of CDKI-73 against DLBCL was assessed in Pfeiffer xenografts. The activity was weaker than expected. Orally-administered 60 mg/kg of CDKI-73 only slightly restrained the growth of subcutaneously Pfeiffer xenografts. Treatment with 80 mg/kg of CDKI-73 resulted in T/C [(mean RTV<sub>treated</sub>)/(mean RTV<sub>vehicle</sub>) $\times$ 100] of 59.36 % at day 17 (Figure 1G).

### CDKI-73 increases H3K27me3 through CDK9 inhibition

Considering the pivotal role of histone modifications in the development and/or progression of DLBCL, we next explored whether CDKI-73 affected the epigenetic modification of histones. We used mass spectrometry (MS) to detect the influence of CDKI-73 on 36 different epigenetic modifications of histone in DLBCL cell line. Notably, we found that treatment with 50 nM CDKI-73 for 24 hours could trigger upregulation of H3K18me1 (1.36-fold) and H3K27me3 (1.29-fold), while the modifications at other sites increased less than 1.20-fold (Figure 2A). In addition, the modification of some sites were suppressed, such as H3K27ac, which was downregulated 0.42-fold, ranked first in all downregulated sites (Figure 2A and *Online Supplementary Table S1*). In accordance with the MS profiling data, Flavopiridol and CDKI-73 all dramatically elevated the level of H3K27me3 accompanied by the upregulation of both H3K27me1 and H3K27me2 levels at the same site in DLBCL cells in Western blot analysis (Figure 2B and *Online Supplementary Figure S1A*). Meanwhile, CDKI-73 treatment did not remarkably alter other well-studied methylation sites on histone H3, including H3K36, H3K79 and H3K9 (Figure 2B and *Online Supplementary Figure S1A* and *Table S1*). To further dissect if CDKI-73 can influence H3K27me3 binding and how CDKI-73 alters the chromatin landscape of DLBCL cells, ChIP-seq was used to analyse the profile distribution of H3K27me3. As expected, we found a global up-regulation of H3K27me3 following CDKI-73 treatment for 24 hours (Figure 2C). Consistently, the transcription of the genes repressed by H3K27me3, *GATA4*,<sup>22</sup> *CDKN2A*,<sup>23,24</sup> *HOXC8*,<sup>25</sup> and *TNFRSF21*,<sup>14</sup> was dramatically decreased (Figure 2D). All of these results indicated that CDKI-73

indeed elevated H3K27me3 in DLBCL.

Next, we attempted to determine the detailed mechanism underlying CDKI-73-induced H3K27me3 upregulation. We observed the upregulation of H3K27me3 along with the decline of MCL1 by other CDK9-specific inhibitors SNS-032, AT-7519, and Dinaciclib (Figure 2E). Furthermore the specific CDK4/6 inhibitor PD0332991 did not influence the level of H3K27me3 (Figure 2F). Then, we hypothesized that the upregulation of H3K27me3 is due to CDK9 inhibition. The lack of selectivity against other CDK of these small molecules led us to further confirm the mechanism by using specific RNA interference. As expected, only CDK9 depletion by RNA interference notably increased H3K27me3 in DLBCL cells, associated with the decline of MCL1 (Figure 2G). No change of H3K27me3 was displayed after CDK1, CDK2, CDK4 and CDK7 depletion (Figure 2H). Further, the transcription of the H3K27me3-targeted genes was also decreased in CDK9 silencing cells (Figure 2I). As the MS assay showed a down-regulation of H3K27ac (Figure 2A), we then investigated whether the decrease of H3K27ac is in response to CDK9 inhibition since the loss of H2K27ac may link to the increase in H3K27me3.<sup>26</sup> To our surprise, the level of H3K27ac, which declined after treatment with CDKI-73, remained unchanged in CDK9 knock-down cells (*Online Supplementary Figure S1C-D*). The detail mechanism of H3K27ac downregulation needs to be further studied and may be due to other CDK inhibition other than CDK9. These data strongly suggested that CDK9 inhibition indeed increased the level of H3K27 trimethylation in DLBCL cells.

H3K27 methylation has been shown to be catalyzed by EZH2,<sup>10</sup> while the demethylation is catalyzed by UTX and JMJD3.<sup>11</sup> We therefore tried to identify the protein regulated by CDK9 to adjust H3K27 methylation. As mentioned before, CDK9 has been shown to participate in transcriptional processes, therefore reducing protein expression by CDK9 inhibition is the most important proposed mechanism. As expected, the mRNA and protein levels of demethylases (UTX and JMJD3) decreased after the treatment with CDK9i in a dose- and time-dependent manner (Figure 3A-B). UTX and JMJD3 almost were completely depleted when the cells were exposed for 24 hours to 0.05  $\mu$ M and 0.1  $\mu$ M CDKI-73/Flavopiridol, respectively (Figure 3B and *Online Supplementary Figure S2A*). To our surprise, the expression of methyltransferases, EZH2, EED, and SUZ12 was also lowered. However, these two CDK9i resulted in the decline of protein and mRNA levels of UTX and JMJD3, especially JMJD3, at lower doses and at early time points of treatment. Methyltransferases were almost completely depleted after treatment with 0.4  $\mu$ M CDKI-73/Flavopiridol for 24 hours. As expected, the silencing of CDK9 and other three CDK9i (SNS-032, AT-7519, and Dinaciclib) also diminished JMJD3, UTX, and PRC2, but the effect on JMJD3 and UTX was more significant (Figure 3A-C). These data demonstrated that H3K27me3 stimulated by CDKI-73 was dependent on CDK9 inhibition.

Previous studies have indicated that CDK1- and CDK2-dependent phosphorylation of EZH2 can influence the methylation of H3K27.<sup>27,28</sup> However, we found no obvious change of EZH2 phosphorylation after treatment with the indicated dose of CDKI-73 (*Online Supplementary Figure S2B*).

**EZH2i reversed the upregulation of H3K27me3 evoked by CDKI-73 and causes a synergistic effect in DLBCL**

It has been reported that down-regulation of H3K27me3 expression by EZH2i has marked anti-tumor potency in

EZH2 mutant (mut) DLBCL preclinical models.<sup>14</sup> Therefore, CDKI-73 improved H3K27me3 expression, which may attenuate its anti-tumor activity against DLBCL. This inspired us to explore whether EZH2i could

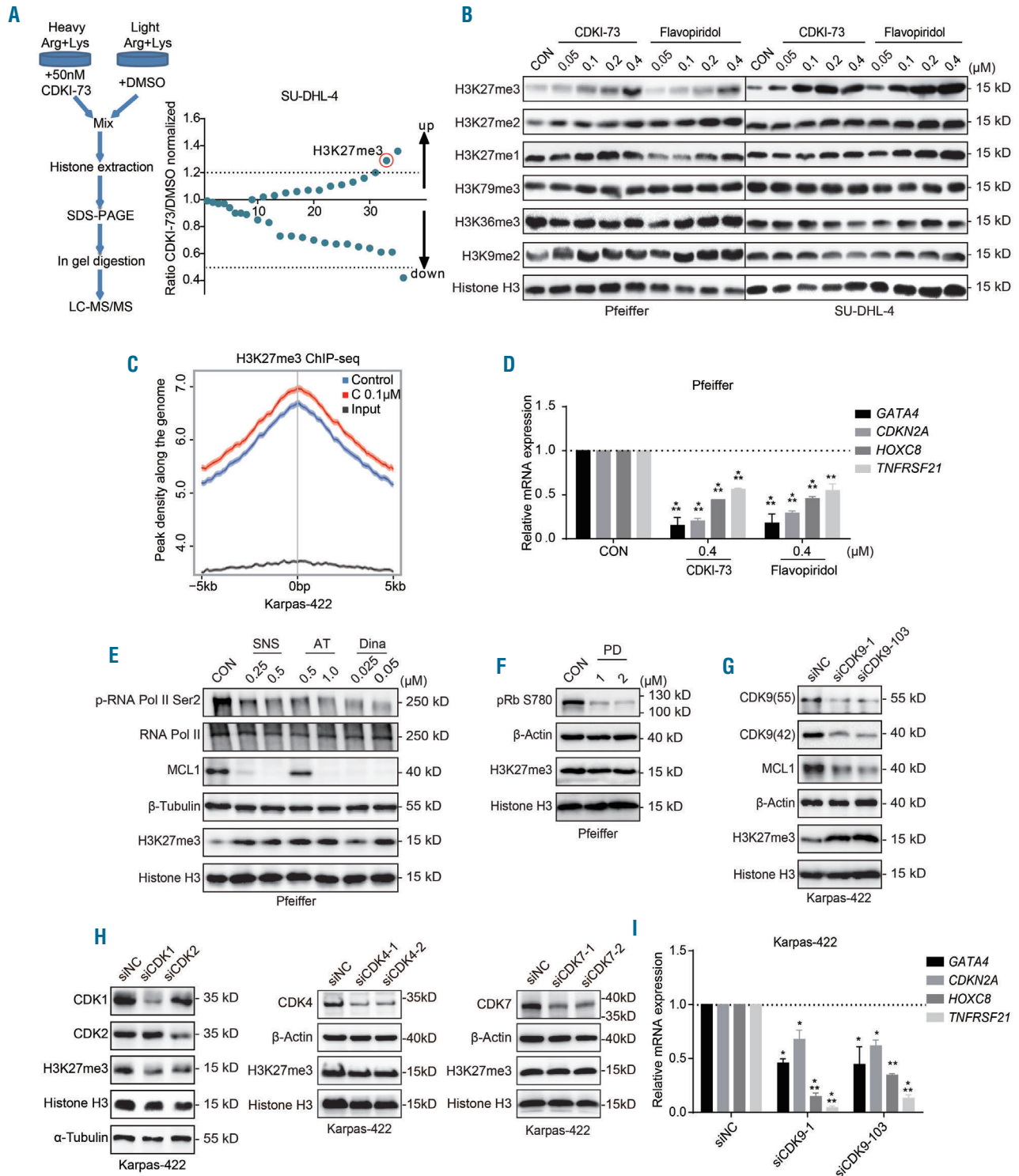


**Figure 2. CDKI-73 induces H3K27me3 via CDK9 inhibition.** (A) Mass Spectrometry assay (MS). Graphical illustration of MS process (left) and normalized CDKI-73/DMSO ratio of 36 loci (right). H3K27me3 is labeled in the red circle. (B) Methylation level of histone in Pfeiffer and SU-DHL-4 cells after treated with CDKI-73/Flavopiridol for 24 hours (h). (C) Summary of ChIP-seq H3K27me3 peaks in the CDKI-73 (red) and control (blue) samples. "0bp" in X-axis indicates the H3K27me3 peak center. (D) The relative mRNA levels of H3K27me3 target genes *GATA4*, *CDKN2A*, *HOXC8*, and *TNFRSF21* in Pfeiffer when cells were treated with CDKI-73/Flavopiridol for 6 h. The influence of CDK9i (E) CDK4/6 inhibitor (F) and CDK9 (G) CDK1, CDK2, CDK4, CDK7 knock-down (H) on the protein level of H3K27me3. (I) The relative mRNA levels of *GATA4*, *CDKN2A*, *HOXC8*, and *TNFRSF21* in CDK9 depletion Karpas-422 cells. C: CDKI-73; SNS: SNS-032; AT: AT-7519; Dina: Dinaciclib; PD: PD0332991. All data are representative of at least three independent experiments. \*\*\**P*<0.001, \*\**P*<0.01, \**P*<0.05 compared with the control group.

reverse the upregulation of H3K27me3, and then synergize the antitumor effect of CDKI-73. As expected, specific EZH2i, EPZ6438 or GSK126 exactly reversed the augmented H3K27me3 evoked by CDKI-73 (Figure 4A). Furthermore the transcription of all these four examined target genes of H3K27me3 was reactivated in co-treated cells compared with cells treated with CDKI-73 alone (Figure 4B). Next, we investigated whether EZH2i could potentiate the anticancer activity induced by CDKI-73. For this, DLBCL cell lines (Will-1, U2932, Karpas-422, SU-DHL-4, Pfeiffer, and SU-DHL-6) were treated with CDKI-73 alone, or in combination with EPZ6438/GSK126 for 72 hours. The combination effect was evaluated using the CI

value according to the CalcuSyn software.<sup>20</sup> The effect is usually considered as synergistic when the CI value is less than 0.8, additive when the CI value is between 0.8-1.2, and antagonistic when the CI value is above 1.2.<sup>20</sup> In EZH2 mut cell lines, Pfeiffer (A677G), SU-DHL-4 (Y641S), Karpas-422 (Y641F), and SU-DHL-6 (Y641N), the average CI values were all below 0.8 (Figure 4C), indicating a synergistic interaction between CDKI-73 and EZH2i in EZH2 mut DLBCL cells. We also found that the IC<sub>50</sub> for EZH2i was lower in CDK9 knock-down cells compared with parent Pfeiffer cells (*Online Supplementary Figure S3A*). However, in Will-1 and U2932 cells, which harbor wild-type (*wt*) EZH2, the combination with EZH2i didn't signif-

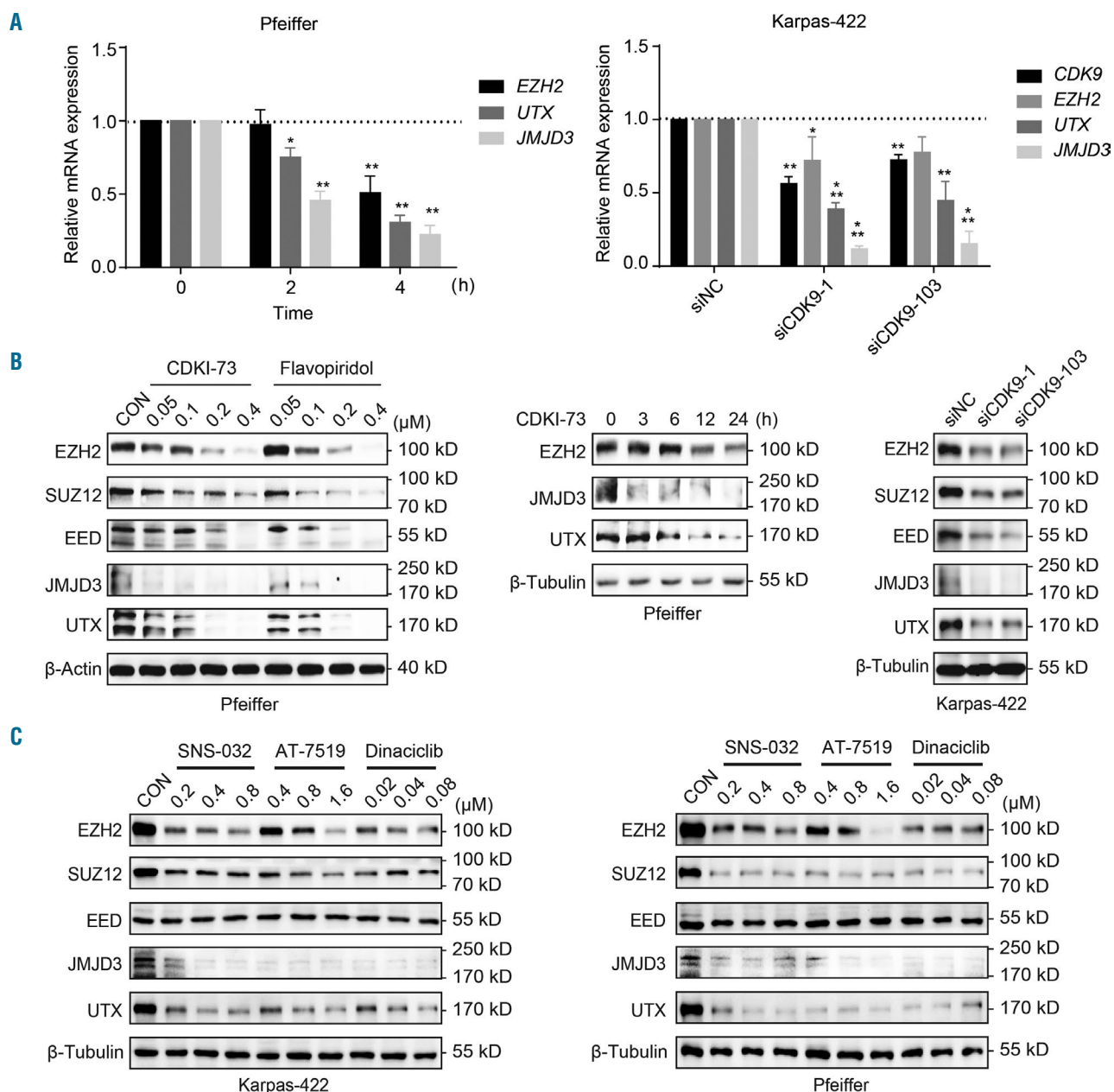


**Figure 3. Transcriptional repression contributed to H3K27me3 elevation via CDK9 inhibition.** (A) The relative mRNA levels of H3K27-related methyltransferases and demethylases after exposure to 0.1 μM CDKI-73 for 2 and 4 hours (h) or siCDK9. (B-C) The protein levels of H3K27-related methyltransferases and demethylases after exposure to CDKI-73/Flavopiridol, other cyclin-dependent kinases (CDK) inhibitors or siCDK9. All data are representative of at least three independent experiments. \*\*\* $P < 0.001$ , \*\* $P < 0.01$ , \* $P < 0.05$  compared with the control group.

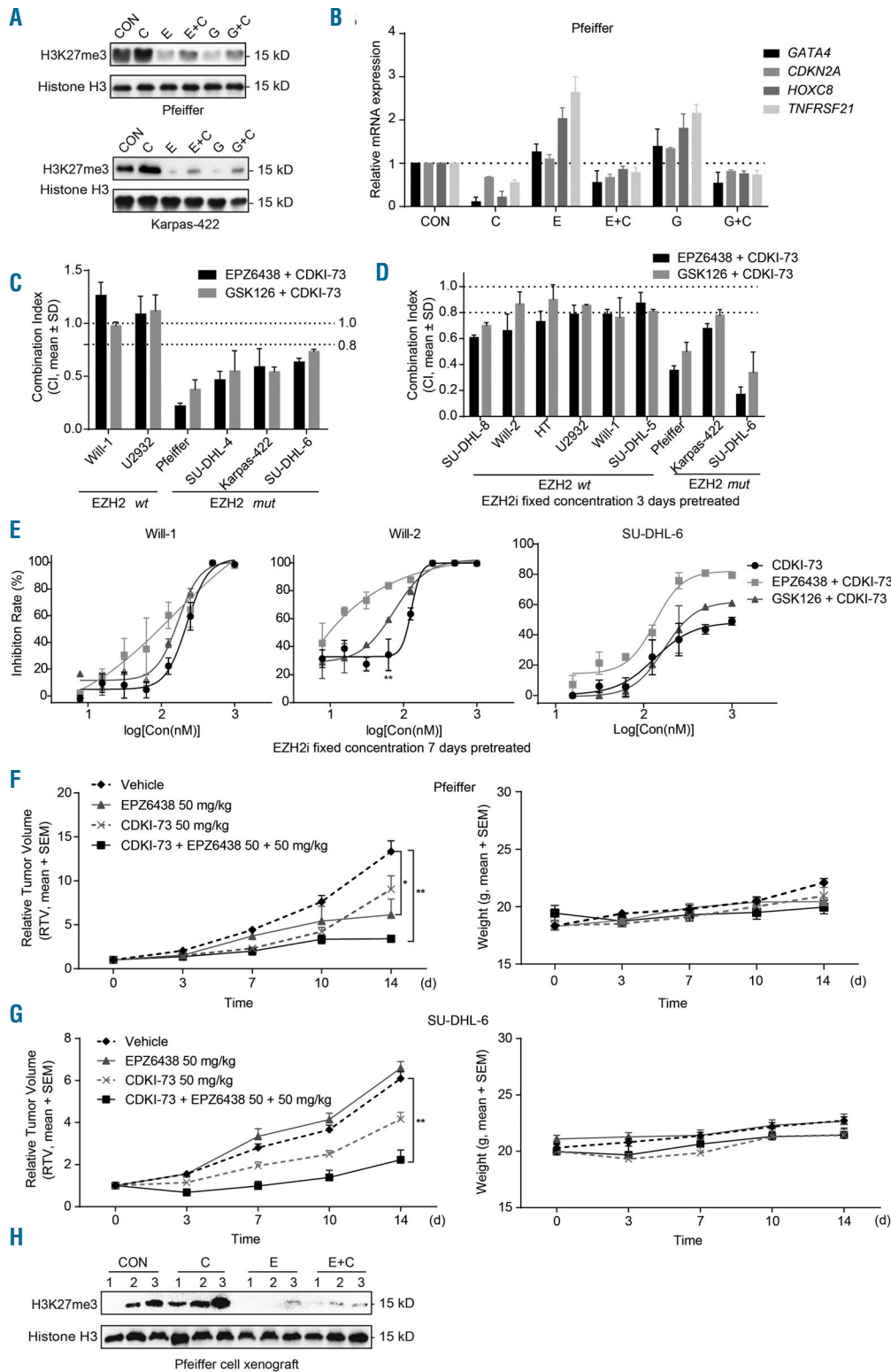


**Figure 4. Combined anti-tumor effect of CDKI-73 and EPZ6438/GSK126 *in vitro* and *in vivo*.** (A) The level of H3K27me3 in Pfeiffer and Karpas-422 cells after treated with CDKI-73, and EPZ6438/GSK126 alone or in combination. Cells were pretreated with 0.5  $\mu$ M EPZ6438/GSK126 alone for 24 hours (h), and then treated in combination with 0.1  $\mu$ M CDKI-73 for an additional 24 h. (B) The relative mRNA levels of *GATA4*, *CDKN2A*, *HOXC8*, and *TNFRSF21* in Pfeiffer cells when pretreated with 0.5  $\mu$ M EPZ6438/GSK126 alone for 24 h, then treated in combination with 0.1  $\mu$ M CDKI-73 for additional 6 h. (C) Average combination index (CI) values. Diffuse large B-cell lymphoma (DLBCL) cells were treated with different doses of CDKI-73 and EPZ6438/GSK126 alone or in combination for 72 h. (D) The CI values of nine different DLBCL cell lines. The combination groups were pretreated with a fixed dose of EPZ6438 or GSK126 for 72 h and then both CDKI-73 and combination groups were treated with increasing doses of CDKI-73 for additional 72 h. (E) The dose-response curves of Will-1, Will-2, and SU-DHL-6 cell lines. The combination groups were pretreated with a fixed dose of EPZ6438 or GSK126 for seven days and then both CDKI-73 and combination groups were treated with increasing doses of CDKI-73 for additional 72 h. (F-G) Relative tumor volume (RTV) and average body weight of nude mice treated with 50 mg/kg CDKI-73 and 50 mg/kg EPZ66438 alone or together with inoculated Pfeiffer and SU-DHL-6 cells. Data are expressed as the mean + standard error of the mean (SEM). (H) The level of H3K27me3 detected in Pfeiffer xenografts at the end of the *in vivo* experiment. C: CDKI-73; E: EPZ6438; G: GSK126. All data are representative of at least three independent experiments. \*\*\* $P < 0.001$ , \*\* $P < 0.01$ , \* $P < 0.05$ . Mut: mutant; wt: wild-type.

icantly improve the anti-proliferative activity of CDKI-73 in this scheme, with CI values higher than 0.8.

As EZH2i takes longer to exhibit weak proliferation inhibition in EZH2 wt cells in the *in vitro* assay,<sup>14</sup> we tried another combination scheme in a panel of DLBCL cell lines. The combination groups were pretreated with a fixed dose of EPZ6438/GSK126 for 72 hours, which was adequate to inhibit H3K27me3, and had no obvious proliferation inhibition (the inhibitory rate was controlled below 20%). The mean CI values of treatment with CDKI-73 and EZH2i were calculated as reported<sup>29</sup> and were also observed to be less than 0.8 in EZH2 mut DLBCL cells (Figure 4D). Even more gratifying was the observation that at least an additional effect was exhibited in SU-DHL-8, Will-1, Will-2, HT, SU-DHL-5, and U2932 cell lines which harbor wt EZH2 (Figure 4D), indicating that EZH2i can promote the anti-proliferative potency of CDKI-73 against DLBCL cell lines with the combination schedule regardless of the EZH2 phenotype. When the pretreatment time with EZH2i was extended to seven days (the inhibitory rate of EZH2i was still controlled below 20%), the dose-response curves of all the co-treatment groups were apparently shifted to the left compared with the curves treated with CDKI-73 alone in EZH2 wt DLBCL cells, also indicating a synergistic effect (Figure 4E).

Thereafter, we evaluated whether EZH2i could enhance the anti-tumor ability of CDKI-73 *in vivo*. In Pfeiffer xenografts, CDKI-73 and EPZ6438 alone suppressed tumor growth compared to the vehicle, yielding a T/C rate of 67.69% and 46.07%, respectively. Combinatorial CDKI-73 and EPZ6438 therapy more potently inhibited tumor growth compared to treatment with CDKI-73, EPZ6438, and vehicle alone, yielding a T/C rate of 25.69%, indicating 74.31% inhibition of tumor growth (Figure 4F). Moreover, there was no obvious weight loss under the combined regimen as compared to the single treatments (Figure 4F). Similar results were observed in another model, SU-DHL-6 (Figure 4G). The superior *in vivo* anti-tumor activity of the combination therapy was also associated with a greater decline in H3K27me3, which was upregulated by CDKI-73 alone (Figure 4H).

### Combination therapy synergistically induces apoptosis and DNA damage

As mentioned above, CDKI-73 alone induced apoptosis and DNA DSB in DLBCL, we next determined the combined effects on apoptosis and DNA damage. As expected, combination treatment remarkably increased the rate of apoptosis compared to each agent alone (Figure 5A). This was associated with a synergistic increase in the PARP cleavage, and a decline of anti-apoptotic proteins including MCL1, XIAP, and BCL-XL (Figure 5B). Similar results were obtained in the *in vivo* assay (Figure 5C). In addition, accumulating data suggest that EZH2 also participates in modulating the DNA damage response.<sup>30</sup> Therefore, we hypothesized that co-induction of DNA damage may be another mechanism contributing to the synergistic anti-tumor effect of the combination. As expected, both comet assay and  $\gamma$ -H2AX analysis indicated that CDKI-73 or EPZ6438/GSK126 alone could induce DNA damage both in Pfeiffer and SU-DHL-4 cells. However, the combined therapy resulted in a dramatic increase in  $\gamma$ H2AX accumulation, and the frequent appearance and expanding volume of comet tails (Figure 5D-E).

### CDK9 and EZH2 inhibition also exhibited synergistic antitumor activity in multiple solid tumors

We further studied whether the combination therapy was also effective against solid tumors. At first, we found that CDKI-73/Flavopiridol elevated H3K27me3 in various kinds of cancer cells, including MCF-7 (breast cancer), MDA-MB-453 (breast cancer), SGC-7901 (gastric cancer), and SW620 (colorectal cancer) (*Online Supplementary Figure S1A*). This finding might partially explain the observation that the inhibition of CDK9 is insufficient to inhibit tumor growth in clinical trials.<sup>31</sup> And as expected, EZH2i down-regulated the augmented H3K27me3 levels induced by CDK9 inhibition and synergized with CDK9i in these solid tumor models *in vitro* and *in vivo* (Figure 6 and *Online Supplementary Figure S3B*). We also found that depletion of both CDK9 and EZH2 in MCF-7 cells delayed cells proliferation, as compared with siCDK9 alone (*Online Supplementary Figure S3C*). And the deletion of CDK9 also diminished PRC2, JMJD3, and UTX, leading to the observed increase of H3K27me3 in these cells (Figure 6E). All these data strongly suggested that CDK9 and EZH2 inhibition also exhibit synergistic interaction in multiple solid tumors.

### Discussion

The frequent observance of resistance and relapse to first line therapy by DLBCL underscores the need for novel approaches to treat this disease. CDKI-73, as an example of a highly efficacious CDK9 inhibitor, has displayed potent anti-tumor activity *in vitro* and *in vivo*.<sup>15-17</sup> Previous studies also have shown that this agent had little toxicity on normal T and B cells while exhibiting potent efficiency against CLL,<sup>15</sup> suggesting it to be a far superior therapeutic agent for clinics. Here, we demonstrated that it retains efficacy in DLBCL *in vitro* and *in vivo*. CDKI-73 exhibited a broad ability to trigger apoptosis and dramatically repress the proliferation of 15 DLBCL cell lines, associated with lost MCL1 and XIAP proteins, owing to CDK9 inhibition. All these data provide a basis for moving forward with the clinical evaluation of CDKI-73 in DLBCL.

Deregulation of CDK has been used to develop antitumor target for more than 20 years. Although CDK inhibitors have always shown tremendous preclinical activity, their clinical application was limited by modest efficacy along with various side effects.<sup>31</sup> Here, in our study, we provided a view of 'CDK9-histone modification crosstalk', which expands the function of CDK9. We found that CDK9 inhibition specifically elevated the trimethylation of H3K27, which may restrain the antitumor potency against DLBCL and other solid tumor types. H3K27me3 is a transcription-repressing epigenetic modification that has been causally associated with the initiation and development of multiple tumor types, especially DLBCL. Recently, oncogenic heterozygous mutations were identified in the SET domain of EZH2 in DLBCL patients, which could elevate H3K27me3, and drive cell proliferation.<sup>14</sup> Moreover, selective EZH2i show preclinical and clinical efficiency against DLBCL by reducing the level of H3K27me3. Positive interim efficacy data from an ongoing phase II clinical trial of EPZ6438, as a single-agent treatment for patients with relapsed or refractory DLBCL, were released at the International Conference on Malignant Lymphoma (Lugano, Switzerland). An objec-

tive response rate of 17 % further provides a strong rationale for the inhibition of H3K27me3 to be a useful therapeutic strategy in DLBCL. Therefore, we used EZH2i for investigating their synergistic effect with CDK9i. As expected, EPZ6438/GSK126 reversed the elevated H3K27me3 triggered by CDK9i and reactivated the transcription of target genes, which was suppressed by H3K27me3. Also, apoptosis induced by the co-treatment was remarkable without reaching the dosages that induce obvious apoptosis by CDKI-73 or EZH2i alone, indicating

strong efficacy with less toxicity at the same time. In addition, combination therapy also improved DNA damage compared to the single treatments alone and synergistically restrained DLBCL growth. More importantly, other CDK9 inhibitors in combination with EZH2i also resulted in a strong synergistic effect in all cases. By expanding our studies with this combination therapy to other solid tumors, in which EZH2i alone do not show any effect, we also demonstrated an impressive synergistic effect. Both preclinical and clinical evidences suggest that only very

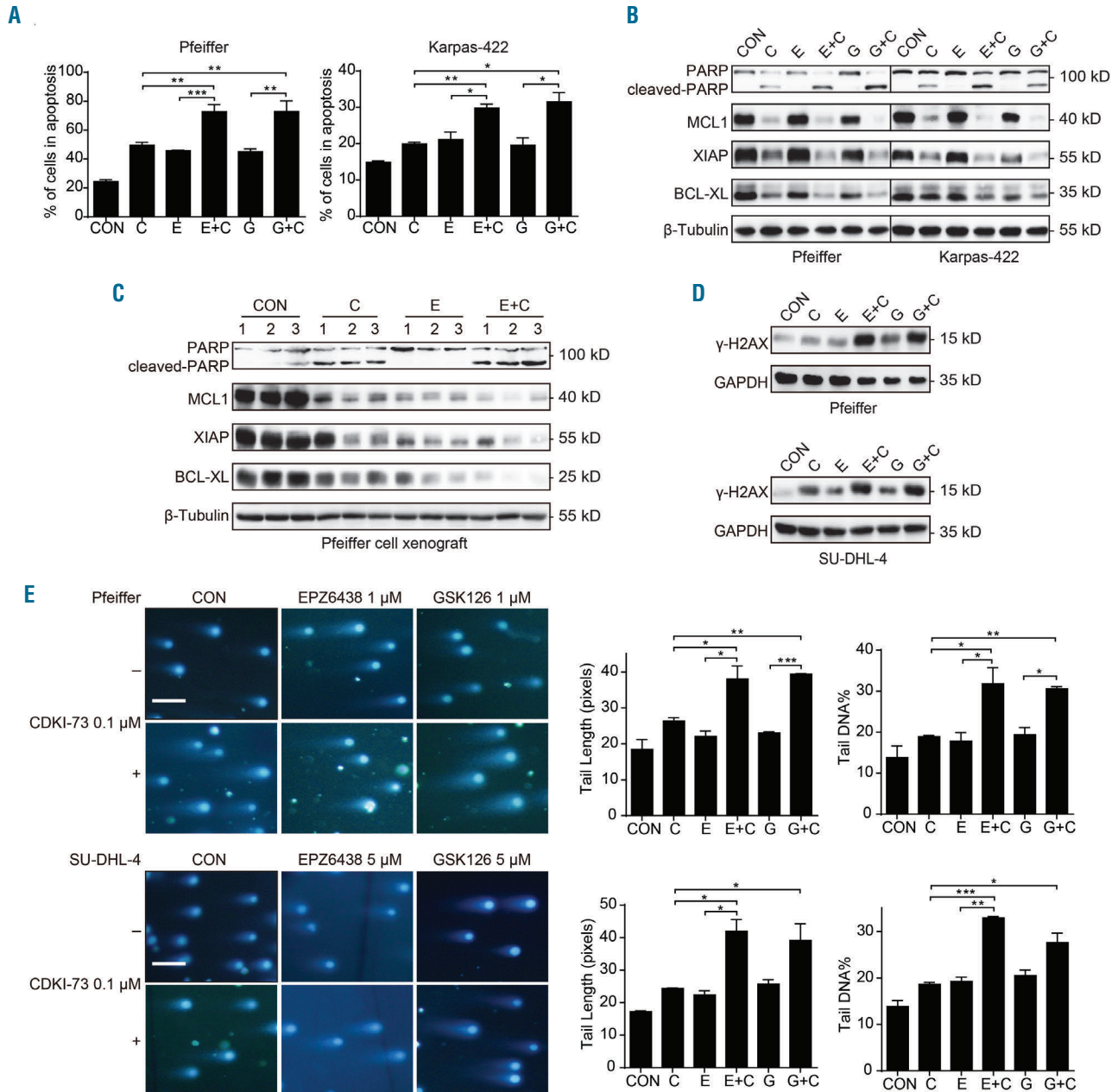


**Figure 5. The combined effect of CDKI-73 and EPZ6438/GSK126 on apoptosis and DNA damage.** (A-B) Quantitative assessment of apoptosis and the expression of apoptosis-related proteins in Pfeiffer and Karpas-422 cells pretreated with EPZ6438/GSK126 alone for 48 hours (h) and then together with CDKI-73 for another 24 h. (C) The level of apoptosis-related proteins detected in Pfeiffer xenografts at the end of the *in vivo* experiment. (D)  $\gamma$ -H2AX detection in Pfeiffer and SU-DHL-4 cells pretreated as mentioned in Figure 4A. (E) Comet assay. Cells were pretreated with EPZ6438/GSK126 alone for 24 h and then in combination with CDKI-73 for additional 24 h (scale bar, 25  $\mu$ m). C: CDKI-73; E: EPZ6438; G: GSK126. All data are representative of at least three independent experiments. \*\*\* $P$ <0.001, \*\* $P$ <0.01, \* $P$ <0.05.

small sets of cancers indeed benefited from EZH2-targeted therapies. Therefore, this study may also open opportunities for EZH2i in solid tumor.

Keeping in mind the important role of the methylation of H3K27 in tumor progression, we also tried to explore the detailed mechanism stimulating H3K27me3 by CDKI-73. In some studies CDK has been linked to H3K27

methylation. CDK1 and CDK2 have been reported to phosphorylate EZH2 at Thr350 and it is considered to be essential for the maintenance of H3K27me3 marks through cell division.<sup>27</sup> Additionally, Thr487 is another residue of EZH2 that can be phosphorylated through activation of CDK1, disrupting EZH2 binding with other PRC2 components, thereby resulting in a decline of

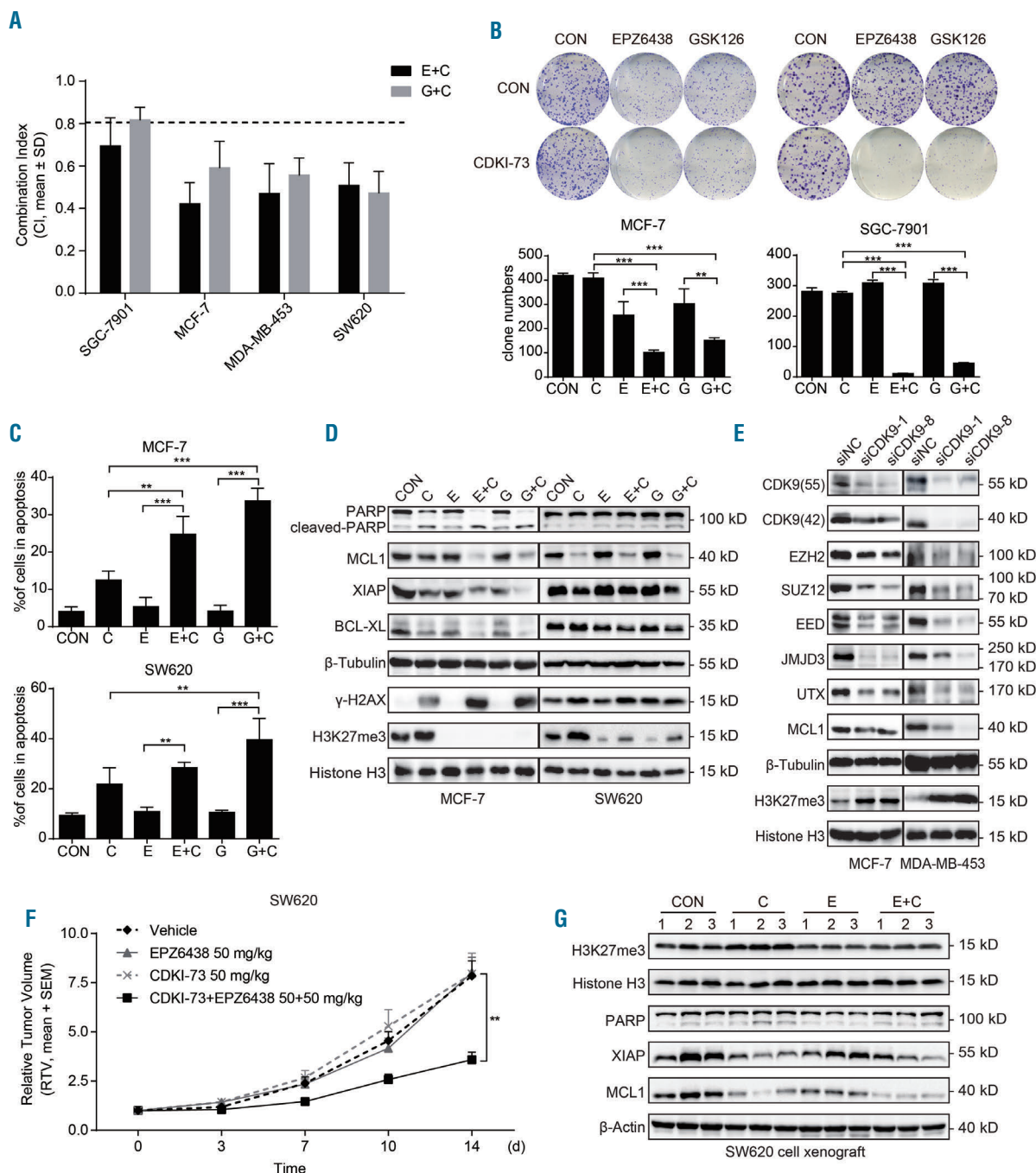


**Figure 6. The combined effect of CDK9 and EZH2i in multiple solid tumors.** (A) The average combination index (CI) values. SGC-7901, MCF-7, MDA-MB-453 and SW620 cells were treated as mentioned in Figure 4D. (B) The combination of CDKI-73 and EZH2i inhibited MCF-7 and SGC-7901 colony formation. (C-D) Quantitative assessment of apoptosis and the expression of apoptosis-related proteins, H3K27me3 and  $\gamma$ -H2AX in MCF-7 and SW620 cells pretreated with EPZ6438/GSK126 for 48 hours (h) and then in combination with CDKI-73 for additional 24 h. (E) H3K27me3, and its related methyltransferases and demethylases level in MCF-7 and MDA-MB-453 cells after siCDK9. (F) Relative tumor volume (RTV) and average body weight of nude mice treated with 50 mg/kg CDKI-73 and 50 mg/kg EPZ6438 alone or together with inoculated SW620 cells. Data are expressed as the mean + standard error of the mean (SEM). (G) H3K27me3 and apoptosis-related proteins level in SW620 xenografts at the end of the in vivo experiment. C: CDKI-73; E: EPZ6438; G: GSK126. All data are representative of at least three independent experiments. \*\*\* $P < 0.001$ , \*\* $P < 0.01$ , \* $P < 0.05$ .

H3K27me3.<sup>28</sup> In our case, CDKI-73 did not change the EZH2 phosphorylation status. The elevated H3K27me3 is related to multiple factors, such as the amplification of EZH2 or another subunit of PRC2 and so on, in numerous tumor types.<sup>12</sup> In addition, inactivation of UTX or JMJD3, resulting in the enrichment of H3K27me3, also has been detected in many kinds of cancers.<sup>32,33</sup> In the present study, surprisingly, the expression of H3K27me3 increased while EZH2 decreased after treatment with CDKI-73/Flavopiridol. Therefore, we paid more attention to the demethylases. Both the protein and mRNA levels of UTX and JMJD3 decreased earlier and more dramatically than EZH2, EED, and SUZ12 when exposed to CDK9i. Moreover, as expected, knock-down of CDK9 also elevated H3K27me3 and decreased the level of JMJD3/UTX

more evidently than that of EZH2. Thus, we speculate that CDK9 inhibition reduced the expression of JMJD3/UTX more powerfully than that of EZH2, leading to H3K27me3 elevation. However, the detailed mechanism of upregulation of H3K27me3 by the loss of CDK9 still needs to be further explored.

In conclusion, we identified that the novel CDK9 inhibitor CDKI-73 exerts a potent anti-tumor activity against DLBCL both *in vitro* and *in vivo*, and represents an attractive therapeutic agent for DLBCL therapy. More importantly, EZH2i in combination with CDK9i results in a strong synergistic effect in DLBCL and other solid tumors by suppressing CDK9 inhibition-stimulated H3K27me3. These data provide a rational basis for the testing of CDK9i in combination with EZH2i in clinical trials.

## References

- Raut LS, Chakrabarti PP. Management of relapsed-refractory diffuse large B cell lymphoma. *South Asian J Cancer*. 2014;3(1):66-70.
- Krystof V, Baumli S, Furst R. Perspective of cyclin-dependent kinase 9 (CDK9) as a drug target. *Curr Pharm Des*. 2012;18(20):2883-2890.
- Wang S, Fischer PM. Cyclin-dependent kinase 9: a key transcriptional regulator and potential drug target in oncology, virology and cardiology. *Trends Pharmacol Sci*. 2008;29(6):302-313.
- Sanchez-Beato M, Sanchez-Aguilera A, Piris MA. Cell cycle deregulation in B-cell lymphomas. *Blood*. 2003;101(4):1220-1235.
- Bellan C, De Falco G, Lazzi S, et al. CDK9/CYCLIN T1 expression during normal lymphoid differentiation and malignant transformation. *J Pathol*. 2004;203(4):946-952.
- Wenzel SS, Grau M, Mavis C, et al. MCL1 is deregulated in subgroups of diffuse large B-cell lymphoma. *Leukemia*. 2012;27(6):1381-1390.
- Gregory GP, Hogg SJ, Kats LM, et al. CDK9 inhibition by dinaciclib potently suppresses Mcl-1 to induce durable apoptotic responses in aggressive MYC-driven B-cell lymphoma *in vivo*. *Leukemia*. 2014;29(6):1437-1441.
- Yecies D, Carlson NE, Deng J, Letai A. Acquired resistance to ABT-737 in lymphoma cells that up-regulate MCL-1 and BFL-1. *Blood*. 2010;115(16):3304-3313.
- Pan G, Tian S, Nie J, et al. Whole-genome analysis of histone H3 lysine 4 and lysine 27 methylation in human embryonic stem cells. *Cell Stem Cell*. 2007;1(3):299-312.
- Kuzmichev A, Nishioka K, Erdjument-Bromage H, Tempst P, Reinberg D. Histone methyltransferase activity associated with a human multiprotein complex containing the Enhancer of Zeste protein. *Genes Dev*. 2002;16(22):2893-2905.
- Hong S, Cho YW, Yu LR, Yu H, Veenstra TD, Ge K. Identification of JmjC domain-containing UTX and JMJD3 as histone H3 lysine 27 demethylases. *Proc Natl Acad Sci U S A*. 2007;104(47):18439-18444.
- McCabe MT, Creasy CL. EZH2 as a potential target in cancer therapy. *Epigenomics*. 2014;6(3):341-351.
- Morin RD, Johnson NA, Severson TM, et al. Somatic mutations altering EZH2 (Tyr641) in follicular and diffuse large B-cell lymphomas of germinal-center origin. *Nat Genet*. 2010;42(2):181-185.
- McCabe MT, Ott HM, Ganji G, et al. EZH2 inhibition as a therapeutic strategy for lymphoma with EZH2-activating mutations. *Nature*. 2012;492(7427):108-112.
- Walsby E, Pratt G, Shao H, et al. A novel Cdk9 inhibitor preferentially targets tumor cells and synergizes with fludarabine. *Oncotarget*. 2014;5(2):375-385.
- Lam F, Abbas AY, Shao H, et al. Targeting RNA transcription and translation in ovarian cancer cells with pharmacological inhibitor CDKI-73. *Oncotarget*. 2014;5(17):7691-7704.
- Xie S, Jiang H, Zhai XW, et al. Antitumor action of CDK inhibitor LS-007 as a single agent and in combination with ABT-199 against human acute leukemia cells. *Acta Pharmacol Sin*. 2016;37(11):1481-1489.
- Shechter D, Dormann HL, Allis CD, Hake SB. Extraction, purification and analysis of histones. *Nat Protoc*. 2007;2(6):1445-1457.
- Huang X, Yan J, Zhang M, et al. Targeting Epigenetic Crosstalk as a Therapeutic Strategy for EZH2-Aberrant Solid Tumors. *Cell*. 2018;175(1):186-199 e119.
- Bijnsdorp IV, Giovannetti E, Peters GJ. Analysis of drug interactions. *Methods Mol Biol*. 2011;731(421-434).
- Yu DS, Cortez D. A role for cdk9-cyclin k in maintaining genome integrity. *Cell Cycle*. 2014;10(1):28-32.
- He A, Shen X, Ma Q, et al. PRC2 directly methylates GATA4 and represses its transcriptional activity. *Genes Dev*. 2012;26(1):37-42.
- Tanaka S, Miyagi S, Sashida G, et al. Ezh2 augments leukemogenicity by reinforcing differentiation blockage in acute myeloid leukemia. *Blood*. 2012;120(5):1107-1117.
- Shi J, Wang E, Zuber J, et al. The Polycomb complex PRC2 supports aberrant self-renewal in a mouse model of MLL-AF9;Nras(G12D) acute myeloid leukemia. *Oncogene*. 2013;32(7):930-938.
- Kim SY, Paylor SW, Magnuson T, Schumacher A. Juxtaposed Polycomb complexes co-regulate vertebral identity. *Development*. 2006;133(24):4957-4968.
- Pasini D, Malatesta M, Jung HR, et al. Characterization of an antagonistic switch between histone H3 lysine 27 methylation and acetylation in the transcriptional regulation of Polycomb group target genes. *Nucleic Acids Res*. 2010;38(15):4958-4969.
- Chen S, Bohrer LR, Rai AN, et al. Cyclin-dependent kinases regulate epigenetic gene silencing through phosphorylation of EZH2. *Nat Cell Biol*. 2010;12(11):1108-1114.
- Wei Y, Chen YH, Li LY, et al. CDK1-dependent phosphorylation of EZH2 suppresses methylation of H3K27 and promotes osteogenic differentiation of human mesenchymal stem cells. *Nat Cell Biol*. 2011;13(1):87-94.
- Li X, Tong LJ, Ding J, Meng LH. Systematic combination screening reveals synergism between rapamycin and sunitinib against human lung cancer. *Cancer Lett*. 2014;342(1):159-166.
- Campbell S, Ismail IH, Young LC, Poirier GG, Hendzel MJ. Polycomb repressive complex 2 contributes to DNA double-strand break repair. *Cell Cycle*. 2014;12(16):2675-2683.
- Asghar U, Witkiewicz AK, Turner NC, Knudsen ES. The history and future of targeting cyclin-dependent kinases in cancer therapy. *Nat Rev Drug Discov*. 2015;14(2):130-146.
- Ezponda T, Licht JD. Molecular pathways: deregulation of histone h3 lysine 27 methylation in cancer-different paths, same destination. *Clin Cancer Res*. 2014;20(19):5001-5008.
- van Haafden G, Dalgliesh GL, Davies H, et al. Somatic mutations of the histone H3K27 demethylase gene UTX in human cancer. *Nat Genet*. 2009;41(5):521-523.